Pathology & Oncology Research | frontiers

TYPE Original Research
PUBLISHED 12 November 2026
DOI 10.3389/pore.2026.1612573

Check for updates

OPEN ACCESS

EDITED BY
Andrea Ladányi,
National Institute of Oncology, Hungary

*CORRESPONDENCE
Neslihan Berker,
neslihan.berker@istanbul.edu.tr

RECEIVED 02 August 2026
REVISED 30 September 2026
ACCEPTED 23 October 2026
PUBLISHED 12 November 2026

CITATION
Berker N, Büyük M, Göksoy B, Serin KR and Güllüoğlu M (2026) Morphologic variants in PanNETs: clinicopathologic and prognostic associations.
Pathol. Oncol. Res. 32:1612573.
doi: 10.3389/pore.2026.1612573

COPYRIGHT
© 2026 Berker, Büyük, Göksoy, Serin and Güllüoğlu. This is an open-access article distributed under the terms of the Creative Commons Attribution License (CC BY). The use, distribution or reproduction in other forums is permitted, provided the original author(s) and the copyright owner(s) are credited and that the original publication in this journal is cited, in accordance with accepted academic practice. No use, distribution or reproduction is permitted which does not comply with these terms.

Morphologic variants in PanNETs: clinicopathologic and prognostic associations

Neslihan Berker [1]*, Melek Büyük [1], Beslen Göksoy [2], Kürşat Rahmi Serin [2] and Mine Güllüoğlu [1]

[1]Department of Pathology, Istanbul Faculty of Medicine, Istanbul University, Istanbul, Türkiye,
[2]Department of General Surgery, Istanbul Faculty of Medicine, Istanbul University, Istanbul, Türkiye

Background: Pancreatic neuroendocrine tumors (PanNETs) exhibit morphologic heterogeneity, including uncommon variant patterns that create diagnostic challenges and whose clinicopathologic significance remains incompletely defined.
Methods: We retrospectively analyzed 82 resected, well-differentiated PanNETs to identify non-classical morphologic variants and evaluate their clinicopathologic and survival associations. Morphologic variants were classified using literature-based criteria. Overall survival and recurrence-free survival were assessed using Kaplan-Meier and Cox models.
Results: Morphologic variants were identified in 20 tumors (24%), including eosinophilic (oncocytic-hepatoid), dyscohesive/plasmacytoid-rhabdoid, lipid-rich, peliotic/angiomatoid, paraganglioid, and pseudoglandular patterns. Variants previously classified as aggressive (n = 14) were significantly associated with higher Ki-67 indices (p = 0.044) and higher WHO grades (p = 0.007). No significant associations were observed between variant status and pathologic stage, nodal status, or metastatic disease at diagnosis. Aggressive variants showed a trend toward shorter overall survival, although this did not reach statistical significance (p = 0.086). In multivariable Cox models for recurrence-free survival, nodal involvement remained independently associated with recurrence risk. The Ki-67 index showed a trend toward increased recurrence risk, although this did not reach statistical significance, whereas morphologic variant status did not show an independent prognostic impact.
Conclusion: Morphologic variants constitute an important component of the histologic spectrum of PanNETs and are associated with adverse histopathologic features. Recognition of these patterns is important in diagnostic practice, especially in limited biopsy or metastatic settings where they may mimic other neoplasms. Given the limited number of variant cases and survival events in this single-institution cohort, their independent prognostic significance remains unproven, and non-classical morphologies should be interpreted cautiously alongside established parameters, such as nodal status and proliferation index.

KEYWORDS
clinicopathologic features, diagnostic pitfalls, morphologic variant, pancreatic neuroendocrine tumor, prognosis

Introduction

Pancreatic neuroendocrine tumors (PanNETs) are a heterogeneous group of well-differentiated neuroendocrine neoplasms that arise in the pancreas, accounting for approximately 2%–5% of all pancreatic tumors. The majority of PanNETs show typical organoid growth patterns, such as trabecular, solid, nested, or glandular architectures. However, these tumors are increasingly recognized as morphologically heterogeneous. Over the past two decades, a growing number of unconventional morphologic variants have been reported, including hepatoid, oncocytic, plasmacytoid/dyscohesive, lipid-rich (clear-cell), paraganglioid, and other rare patterns. The majority of these reports are isolated case reports or small series [1–27].

These variants may mimic other primary pancreatic neoplasms or metastatic tumors, particularly in small biopsy or metastatic specimens, leading to diagnostic challenges. Moreover, accumulating evidence suggests that certain morphologic patterns are associated with distinct clinical behaviors, indicating that morphologic heterogeneity may reflect underlying biological differences in PanNETs.

The most comprehensive systematic evaluation of morphologic variants in PanNETs to date was performed by Xue et al. [1]. In that study, oncocytic, hepatoid, plasmacytoid/dyscohesive, and lipid-rich variants were associated with adverse pathologic features, suggesting that morphologic "aggressiveness" may reflect biologic behavior. However, it remains uncertain whether morphologic variant status offers prognostic information that is independent of established parameters, including tumor grade, Ki-67 index, and nodal status.

In this context, systematic evaluation of well-characterized institutional cohorts may help further define the clinicopathologic relevance of PanNET morphologic variants. In the present study, we retrospectively analyzed 82 resected PanNETs to characterize morphologic variants, determine their prevalence, and examine their clinicopathologic associations and survival observations.

Materials and methods

Case selection and study design

A retrospective analysis was performed on all pancreatic resection specimens diagnosed as well-differentiated neuroendocrine tumors from 2010 to 2024 in our institution's pathology archive. Tumors smaller than 5 mm ("micro-PanNETs") and cases associated with hereditary syndromes (e.g., multiple endocrine neoplasia type 1 or von Hippel-Lindau disease) were excluded from the study. A total of 82 resection cases were identified. For each case, demographic information (age and sex), resection type (Whipple procedure, distal pancreatectomy, or enucleation/enucleation-type excision), tumor location [head/uncinate or distal pancreas (body-tail)], tumor diameter, and lymph node status were retrieved from pathology reports. Pathologic nodal status was assessed only in cases with submitted lymph nodes; cases without lymph node sampling were classified as Nx. The presence of distant metastatic disease at diagnosis was recorded based on available clinical, radiologic, and pathologic data at the time of initial diagnosis or surgery. Cases with indeterminate metastatic status were excluded from the corresponding analyses. Clinical functional status was determined from the available clinical records and was categorized as functional, non-functional, or unavailable. When available, hormone immunohistochemistry performed as part of the routine diagnostic workup was also recorded.

This study was approved by the institutional ethics committee (Approval No. 2025/1270). Due to the retrospective design and the use of anonymized archival material, the requirement for informed consent was waived by the ethics committee.

Histopathologic evaluation and variant classification

All hematoxylin-eosin-stained slides containing tumor tissue were systematically reviewed for deviations from conventional (classical) PanNET morphology, defined as organoid (nested, trabecular, or ribbon-like) architecture composed of relatively uniform tumor cells with finely granular ("salt-and-pepper") chromatin and delicate fibrovascular stroma. Any architectural or cytologic features diverging from this conventional appearance were recorded as non-classical morphologic patterns. Morphologic variant classification was assigned through a consensus review by three pathologists with focused experience in gastrointestinal and hepatopancreatobiliary pathology, using previously published criteria described by Xue et al. [1]. Non-classical patterns were categorized into defined morphologic variants accordingly. The extent of the variant component was estimated as focal (<25%), substantial (25%–75%), or diffuse (>75%), in keeping with this report. Variants were further stratified as more aggressive, less aggressive, or indeterminate according to the prognostic classification proposed in the aforementioned study. For tumors with abundant eosinophilic cytoplasm, additional immunohistochemical markers, such as HepPar-1 and arginase-1, were performed to assess hepatocytic differentiation. S100 immunohistochemistry was performed on cases with paraganglioid morphology to evaluate for the presence of a sustentacular staining pattern, as previously reported in paraganglioid PanNETs [1]. Cytokeratin expression was confirmed in these cases, supporting a diagnosis of PanNET rather than paraganglioma.

The Ki-67 index and corresponding histologic grade were evaluated according to the 2019 WHO (World Health Organization) Classification of Tumors [28]. Areas with the highest nuclear labeling were identified before counting. The Ki-67 index was assessed in hotspot areas by manually counting at least 500 tumor cell nuclei at high power, in line with current recommendations. Pathologic stage was recorded according to the American Joint Committee on Cancer, 8th edition, criteria [29].

Lymphovascular invasion (LVI) and perineural invasion (PNI) were systematically assessed during slide review. In enucleation or limited excision specimens, LVI and PNI were recorded only when unequivocally present; absence of invasion in these specimens was considered not assessable due to limited peritumoral tissue. All tumors had been previously confirmed as neuroendocrine neoplasms by immunohistochemical positivity for at least two neuroendocrine markers (chromogranin A and synaptophysin).

Follow-up and survival analysis

Overall survival (OS) was defined as the time from surgical resection to death from any cause or the last known survival status. Patients who were alive at the time of the last survival status assessment were censored.

Recurrence-free survival (RFS) was defined as the time from surgical resection to the first documented evidence of tumor recurrence, including local recurrence, regional disease, or distant metastasis, whichever occurred first. Recurrence was determined based on available clinical and/or radiologic follow-up data. Patients without documented recurrence were censored on the date of the last available clinical or radiologic follow-up.

Statistical analysis

Because the number of less aggressive and indeterminate variants was limited, statistical analyses were performed by comparing the more aggressive variant group with all remaining cases. The latter group comprised tumors with less aggressive or indeterminate variants, in addition to PanNETs with conventional morphology. For survival analyses, the less aggressive and indeterminate variants were grouped with the conventional tumors in the primary model given the lack of consistent evidence of aggressive behavior and the absence of enrichment for adverse outcomes in our cohort. Sensitivity analyses were conducted by reclassifying variants of uncertain behavior as aggressive. As an additional sensitivity analysis, clinicopathologic and survival analyses were repeated using a ≥50% threshold for variant morphology to assess whether the extent of the variant component influenced the observed associations.

Continuous variables (e.g., Ki-67 index and tumor size) were analyzed using the Mann-Whitney U test due to non-normal distribution. Categorical variables (grade, LVI, PNI, T stage, and N stage) were compared using chi-square tests or exact tests, including the Fisher-Freeman-Halton test for multi-category variables, as appropriate.

Kaplan-Meier analysis with log-rank testing and univariable Cox proportional hazards modeling were performed. Given the limited number of OS events (n = 14), multivariable Cox regression was not undertaken for OS to avoid model overfitting. For RFS (15 events), the multivariable analysis was restricted to a maximum of three clinically selected covariates to maintain an acceptable event-per-variable ratio.

All tests were two-sided, and p-values <0.05 were considered statistically significant. All statistical analyses were performed using SPSS version 31 (IBM SPSS Statistics for macOS).

TABLE 1 Clinicopathologic characteristics of resected well-differentiated pancreatic neuroendocrine tumors (n = 82).

Characteristic	n (%) or median (range)
Age at diagnosis (years)	52.5 (15–77)
Sex	
Female	45/82 (55%)
Male	37/82 (45%)
Tumor size (cm)	2.7 (0.8–14)
Ki-67 index (%)	5 (0.7–53)
Histologic grade (WHO 2019)	
Grade 1	17/82 (21%)
Grade 2	59/82 (72%)
Grade 3	6/82 (7%)
Tumor location	
Head/uncinate	32/82 (39%)
Distal pancreas (body–tail)	50/82 (61%)
Resection type	
Whipple procedure	23/82 (28%)
Distal pancreatectomy	41/82 (50%)
Enucleation/local excision	17/82 (21%)
Total pancreatectomy	1/82 (1%)
Pathologic T stage (AJCC 8th edition)	
T1	32/82 (39%)
T2	28/82 (34%)
T3	15/82 (18%)
T4	3/82 (4%)
Tx	4/82 (5%)
Pathologic N stage	
N0	32/82 (39%)
N1	20/82 (24%)
Nx	30/82 (37%)
Distant metastasis at initial diagnosis	6/79 (8%)
Lymphovascular invasion	35/68 (51%)
Perineural invasion	18/65 (28%)

The number of evaluable cases varies across variables due to missing data. Abbreviations: AJCC, american joint committee on cancer; Tx, primary tumor cannot be assessed; Nx, regional lymph nodes cannot be assessed.

Results

Patient and tumor characteristics

A total of 82 resected PanNETs were included in the study. The cohort consisted of 45 female patients (55%) and 37 male patients (45%), with a mean age at diagnosis of 51.5 ± 13.4 years (range: 15–77). Seventeen tumors (21%) were clinically functional, including 16 clinically diagnosed insulinomas, whereas 61 (74%) were non-functional; functional status was unavailable in 4 cases (5%). Insulin immunohistochemistry was performed in 15 of the 16 clinically diagnosed insulinomas and was positive in all 15.

The surgical procedures included Whipple procedures (n = 23, 28%), distal pancreatectomies (n = 41, 50%), enucleation or local excision (n = 17, 21%), and a total pancreatectomy (n = 1, 1%). The tumors were located in the head/uncinate process in 32 cases (39%) and in the distal pancreas (body-tail) in 50 cases (61%). The median tumor size was 2.7 cm (IQR 1.8-4.1; range, 0.8–14 cm). Tumor size could not be assessed

10.3389/pore.2026.1612573

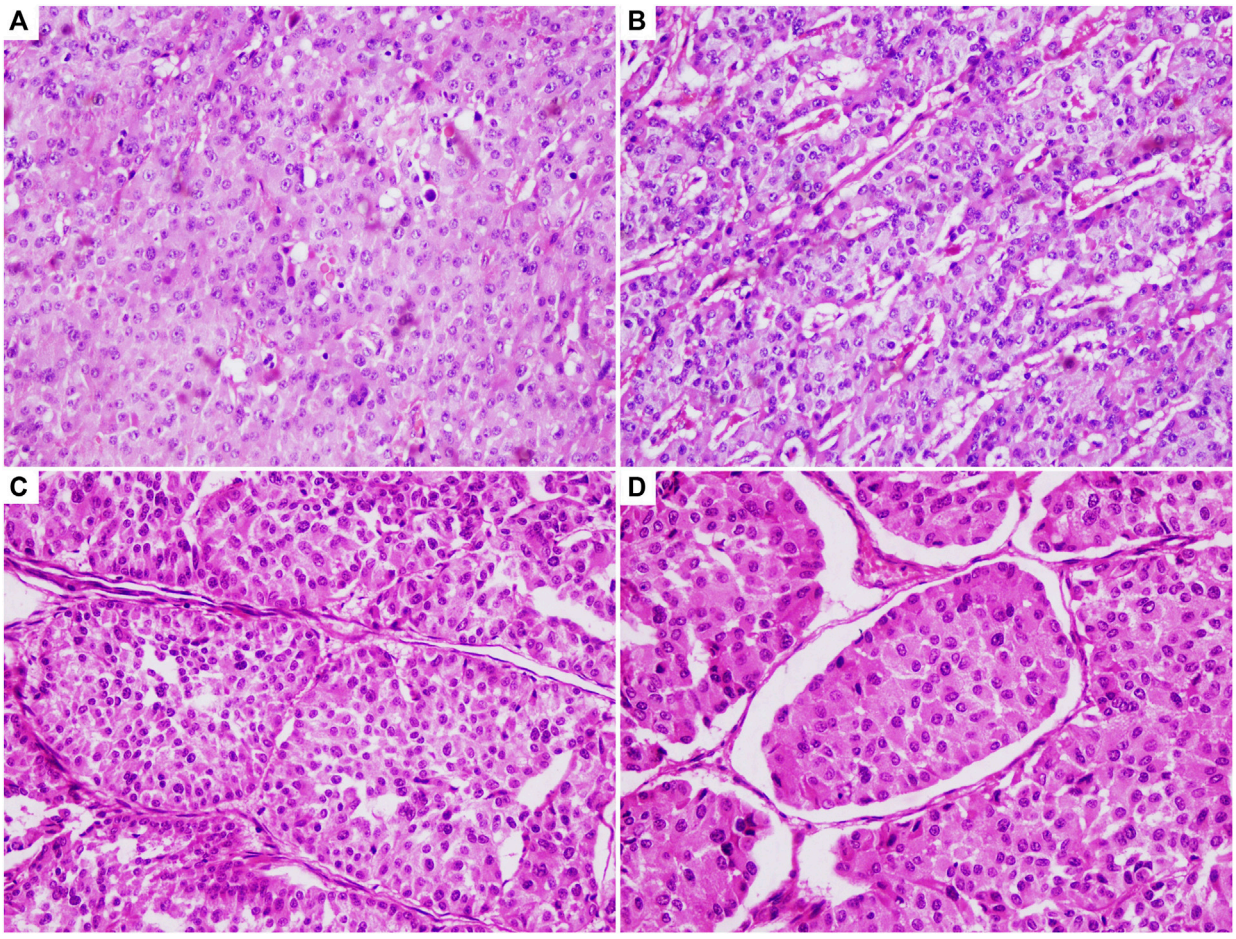


FIGURE 1
Eosinophilic (oncocytic-hepatoid spectrum) variant of a pancreatic neuroendocrine tumor. Representative examples of well-differentiated PanNETs with overlapping oncocytic and hepatoid morphologic features, including abundant granular eosinophilic cytoplasm, solid/trabecular architecture, round to oval nuclei, and variably prominent nucleoli **(A–D)**.

in four consultation cases due to the absence of the original resection specimen and complete pathology documentation; consequently, the pathologic T stage was unavailable for these cases. Among the remaining 78 evaluable tumors, the pathologic T stage was classified as T1 in 32 cases (41%), T2 in 28 cases (36%), T3 in 15 cases (19%), and T4 in 3 cases (4%).

According to the 2019 WHO classification [28], 17 tumors (21%) were grade 1, 59 (72%) were grade 2, and 6 (7%) were grade 3. The median Ki-67 index was 5% (range, 0.7%–53%).

LVI was observed in 35 of the 68 evaluable cases (51%), and PNI was present in 18 out of 65 cases (28%).

Pathologic nodal status was N0 in 32 cases (39%), N1 in 20 cases (24%), and Nx in 30 cases (37%). Distant metastasis at diagnosis was observed in 6 of 79 evaluable cases (8%), all involving the liver.

The clinicopathologic characteristics of resected PanNETs are summarized in Table 1.

Morphologic variants of PanNETs

On histopathologic review, 20 of the 82 tumors (24%) exhibited non-classical morphologic patterns and were classified as morphologic variants, while the remaining cases displayed conventional PanNET morphology. Among the 20 variants, 6 (30%) were eosinophilic (oncocytic-hepatoid spectrum), 6 (30%) were dyscohesive tumors with plasmacytoid/rhabdoid features, 3 (15%) were peliotic/angiomatoid, 2 (10%) were lipid-rich (clear cell), 2 (10%) were paraganglioid, and 1 (5%) was pseudoglandular. One dyscohesive tumor also contained a focal (<25%) hepatoid component, and one paraganglioid tumor exhibited accompanying pleomorphic features. Overall, the variant component was diffuse in 7 cases (35%), substantial in 11 cases (55%), and focal in 2 cases (10%). Notably, 18 of the 20 tumors (90%) demonstrated at least substantial variant involvement. Of the morphologic variants described in the literature, ductuloinsular, mammary tubulo-lobular carcinoma-like, and sclerosing patterns were not identified in this cohort.

Based on the categorization described by Xue et al., eosinophilic (oncocytic-hepatoid), dyscohesive tumors with plasmacytoid/rhabdoid features, and lipid-rich variants were categorized as more aggressive morphologic variants, comprising 14 tumors (17% of the total cohort); pleomorphic and paraganglioid tumors were classified as less aggressive variants, comprising 2 tumors (2%); and pseudoglandular and peliotic/angiomatoid patterns as indeterminate variants, comprising 4 tumors (5%).

10.3389/pore.2026.1612573

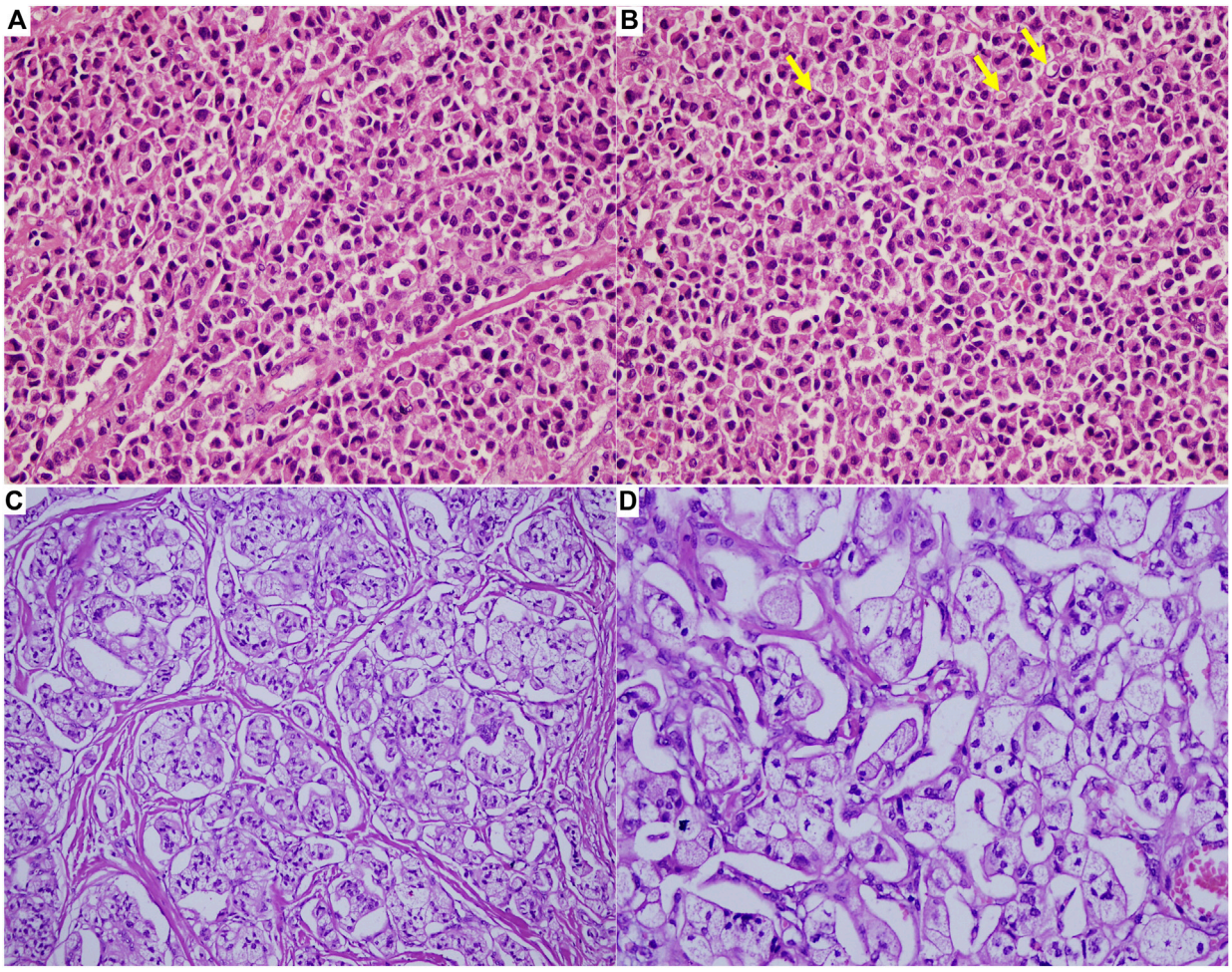


FIGURE 2
Dyscohesive and lipid-rich variants of a pancreatic neuroendocrine tumor. Dyscohesive variant with plasmacytoid/rhabdoid features, showing diffuse, sheet-like growth composed of dyscohesive tumor cells with plasmacytoid to rhabdoid cytomorphology **(A)**. Tumor cells exhibiting eccentric nuclei, occasional nuclear compression, and prominent intracytoplasmic eosinophilic globules (arrows), with focal signet-ring-like and targetoid features **(B)**. Lipid-rich (clear cell) variant, composed of cells with optically clear to finely vacuolated cytoplasm arranged in solid and nested growth patterns, with peripherally displaced nuclei and focal nuclear compression **(C,D)**.

Eosinophilic variant (oncocytic-hepatoid spectrum) (n = 6)

These tumors showed trabecular to solid growth patterns, with tumor cells displaying broad eosinophilic cytoplasm and a relatively low nuclear-to-cytoplasmic ratio, associated with a hepatocytic/oncocytic-like appearance (Figure 1). This component was diffuse in 2 cases, substantial in 3 cases, and focal in 1 case. Hepatocytic marker immunoexpression was variable and generally focal: focal arginase-1 positivity was observed in 2 cases, focal positivity for both HepPar-1 and arginase-1 was observed in 1 case, whereas 4 cases were negative for hepatocytic markers (Supplementary Figure S1).

Dyscohesive variant with plasmacytoid/rhabdoid features (n = 6)

These tumors demonstrated prominent loss of cohesion with a diffuse growth pattern, often forming sheets of discohesive tumor cells that ranged from plasmacytoid to rhabdoid in appearance (Figures 2A,B). Tumor cells showed abundant eosinophilic cytoplasm with variable paranuclear eosinophilic protein inclusions, imparting a rhabdoid or, in some cases, a signet-ring-like morphology. Nuclei were frequently eccentrically displaced and occasionally compressed, resulting in partial or complete obscuration of the characteristic salt-and-pepper chromatin. This pattern was diffuse in 2 tumors, substantial in 3 tumors, and focal in 1 tumor. In addition, one tumor showed a focal hepatoid component (<25%) admixed with predominant plasmacytoid/dyscohesive morphology and was classified within this variant category.

Lipid-rich (clear cell) variant (n = 2)

Tumors classified as lipid-rich variants contained cells with optically clear to vacuolated cytoplasm, resulting in a clear-cell appearance (Figures 2C,D). Involvement was diffuse in one case and substantial in the other. In some otherwise conventional tumors, clear-cell-like changes adjacent to fibrosis related to prior diagnostic fine-needle aspiration mimicked this variant,

10.3389/pore.2026.1612573

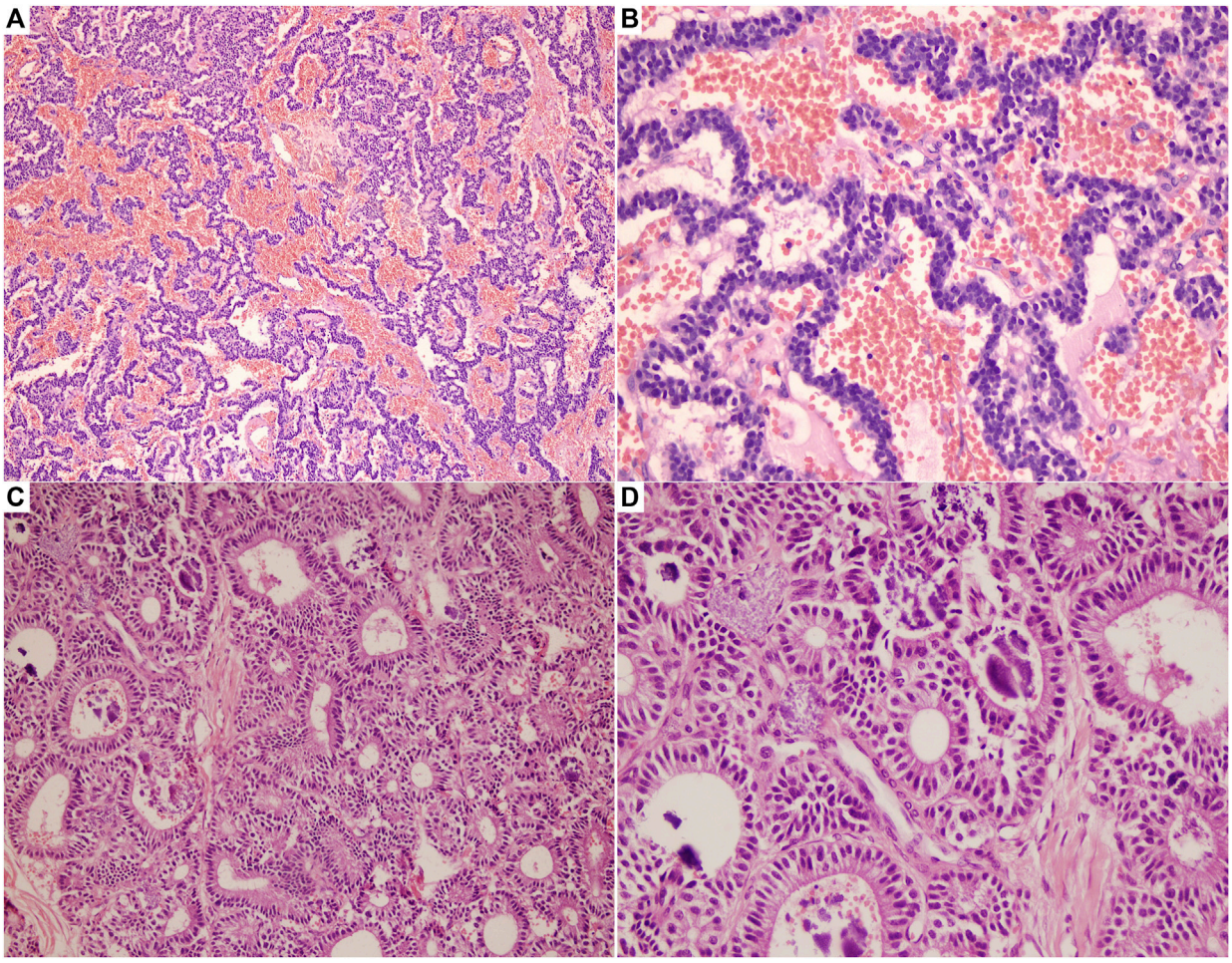


FIGURE 3
Peliotic/angiomatoid and pseudoglandular variants of a pancreatic neuroendocrine tumor. Hematoxylin and eosin-stained sections showing blood-filled peliotic/angiomatoid spaces surrounding and partially obscuring the underlying neuroendocrine tumor cells **(A,B)**. Pseudoglandular variant, characterized by gland-like spaces at low magnification **(C)** and well-formed pseudoglandular structures with focal intraluminal calcifications at higher magnification **(D)**.

representing a potential diagnostic pitfall (Supplementary Figure S2).

Peliotic/angiomatoid variant (n = 3)

This variant was characterized by conspicuous blood-filled spaces and pelioid or angiomatoid change within the tumor (Figures 3A,B). The peliotic/angiomatoid pattern was diffuse in two cases and substantial in one case, a feature that may resemble a vascular lesion, particularly in limited biopsy material.

Pseudoglandular variant (n = 1)

The pseudoglandular variant demonstrated a substantial pseudoglandular component characterized by gland-like spaces within a tumor otherwise composed of neuroendocrine cells, potentially simulating adenocarcinoma, particularly in small samples (Figure 3C). Focal intraluminal calcifications were also present (Figure 3D).

Paraganglioid variant (n = 2)

Paraganglioid tumors showed a Zellballen-like, nested architecture, reminiscent of paraganglioma (Figure 4). This pattern was substantial in both cases. In one case, prominent pleomorphic (symplastic) tumor cells were also observed (Figures 4C,D). In addition, S100 immunostaining showed diffuse positivity within the tumor cells, whereas a peripheral sustentacular staining pattern was not observed (Supplementary Figure S3).

Comparison between aggressive morphologic variants and other tumors (aggressive vs. other group)

The clinicopathologic features of tumors classified as aggressive morphologic variants (n = 14) were compared with those of all remaining cases, including tumors with conventional morphology and less aggressive or indeterminate variants (Table 2).

Aggressive variants were significantly more frequent in male patients compared with the other tumors (79% vs. 38%; $p = 0.008$).

10.3389/pore.2026.1612573

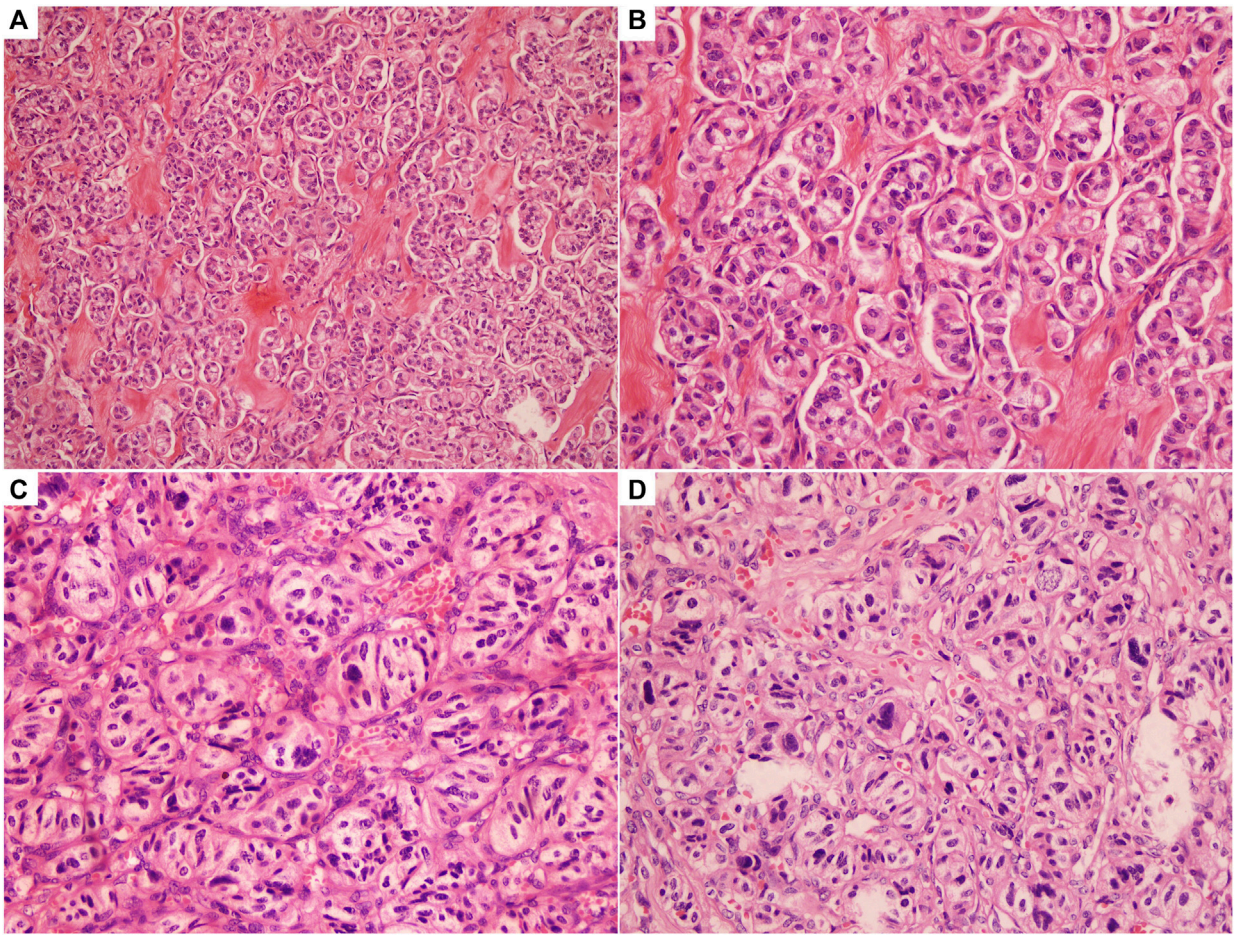


FIGURE 4
Paraganglioid variant of a pancreatic neuroendocrine tumor. Zellballen-like nested architecture with delicate fibrovascular septa in the first case **(A,B)**, and paraganglioid growth with pleomorphic tumor cells and symplastic nuclear atypia in the second case **(C,D)**.

Age and tumor location did not differ significantly between the groups ($p > 0.05$).

Tumors in the aggressive variant group showed a trend toward larger tumor size compared with the other group, although the difference was not statistically significant (median 3.15 cm vs. 2.45 cm; $p = 0.070$). No significant association was identified between aggressive morphologic variants and pathologic T stage (early [T1-T2] vs. advanced [T3-T4]) or pathologic nodal status.

The Ki-67 index was significantly higher in aggressive morphologic variants than in the other tumors (median 9.5% vs. 5%; $p = 0.044$). The mean Ki-67 values were 17.3% and 6.38%, respectively.

The distribution of WHO grades (G1-G3) differed significantly between aggressive morphologic variants and the other tumors ($p = 0.007$). Grade 3 tumors were more frequent in the aggressive group than in the other group (29% vs. 3%). Notably, 4 of 6 grade 3 tumors (67%) belonged to the aggressive group.

LVI and PNI tended to be more frequent in aggressive morphologic variants than in the other tumors (LVI: 71% vs. 46%; PNI: 43% vs. 24%); however, neither difference reached statistical significance. Tumor necrosis was observed in two tumors, both of which belonged to the aggressive dyscohesive variant, and it was not identified in the remaining cases.

Among the six patients with distant metastatic disease at diagnosis, two tumors belonged to the aggressive morphologic variant group, whereas the remaining four were classified as conventional variants. No statistically significant association was identified between morphologic variant status and distant metastatic disease at diagnosis.

In a sensitivity analysis restricted to tumors with ≥50% variant morphology, the association with male sex and higher WHO grade remained significant, whereas the previously observed association with the Ki-67 index was no longer statistically significant. No significant associations were observed with the other clinicopathologic parameters examined.

Survival analyses

Overall survival

Overall survival analyses were performed on the entire cohort, as survival status was available for all patients. The median follow-up duration was 101.6 months.

TABLE 2 Clinicopathologic comparison between aggressive morphologic variants and other pancreatic neuroendocrine tumors.

Parameter	Aggressive	Other	p-value
Age, years	49.5 (30–71)	53.0 (15–77)	0.844
Sex			**0.008**
Male	11/14 (79%)	26/68 (38%)	
Female	3/14 (21%)	42/68 (62%)	
Tumor size, cm	3.15 (1.6–14)	2.45 (0.8–13.5)	0.070
Tumor location			0.381
Head/uncinate	7/14 (50%)	25/68 (37%)	
Distal pancreas	7/14 (50%)	43/68 (63%)	
Ki-67 index, %	9.5 (1–53)	5 (0.7–25)	**0.044**
WHO grade (2019)			**0.007**
Grade 1	3/14 (21%)	14/68 (21%)	
Grade 2	7/14 (50%)	52/68 (76%)	
Grade 3	4/14 (29%)	2/68 (3%)	
Pathologic T stage			0.727
Early (T1–T2)	10/14 (71%)	50/64 (78%)	
Advanced (T3–T4)	4/14 (29%)	14/64 (22%)	
Pathologic N stage			1.000
N0	8/13 (62%)	24/39 (62%)	
N1	5/13 (38%)	15/39 (38%)	
Distant metastasis at initial diagnosis			0.255
Present	2/13 (15%)	4/66 (6%)	
Absent	11/13 (85%)	62/66 (94%)	
Lymphovascular invasion			0.135
Present	10/14 (71%)	25/54 (46%)	
Absent	4/14 (29%)	29/54 (54%)	
Perineural invasion			0.185
Present	6/14 (43%)	12/51 (24%)	
Absent	8/14 (57%)	39/51 (76%)	

Percentages and p-values were calculated based on cases with available data for each variable; therefore, the total number of evaluable cases differs across variables. Statistically significant p-values (<0.05) are shown in bold. Continuous variables are presented as median (range). Values are presented as n (%) unless otherwise indicated.

Overall survival did not differ significantly by morphologic variant status; however, aggressive variants showed a trend toward shorter OS than other tumors (Figure 5, log-rank p = 0.086). In a sensitivity analysis that included indeterminate variants in the aggressive group, no significant difference in OS was observed (log-rank p = 0.459).

In univariable Cox regression analyses, aggressive morphologic variants showed a trend toward an increased risk of death, but the association was not statistically significant (HR 2.66; 95% CI 0.83–8.54; p = 0.099). In contrast, a higher Ki-67 index was significantly associated with worse OS (HR 1.05 per 1% increase; 95% CI 1.02-1.09; p = 0.002). Grade 3 tumors (vs. grade 1–2) (HR 4.18; 95% CI 0.89-19.58; p = 0.069) and nodal involvement (HR 3.42; 95% CI 1.00-11.77; p = 0.051) showed trends toward worse OS, but neither reached statistical significance. Advanced pT stage and tumor size greater than 2 cm were not significantly associated with OS. Consistent with the Kaplan-Meier findings in the sensitivity analysis, variant status defined in this manner was not associated with OS in the univariable Cox regression analysis (HR 1.55; 95% CI 0.48-4.94; p = 0.462).

In an additional sensitivity analysis applying a ≥50% threshold for variant morphology, the survival findings remained unchanged, with no statistically significant difference in OS between aggressive variants and other tumors (log-rank p = 0.069; univariable Cox HR = 2.81, 95% CI 0.88–9.00, p = 0.081).

All univariable Cox regression results are presented in Table 3.

Recurrence-free survival

Recurrence-free survival analysis was performed on 64 patients with available follow-up data, among whom 15 recurrence events were documented. Kaplan-Meier analysis demonstrated no

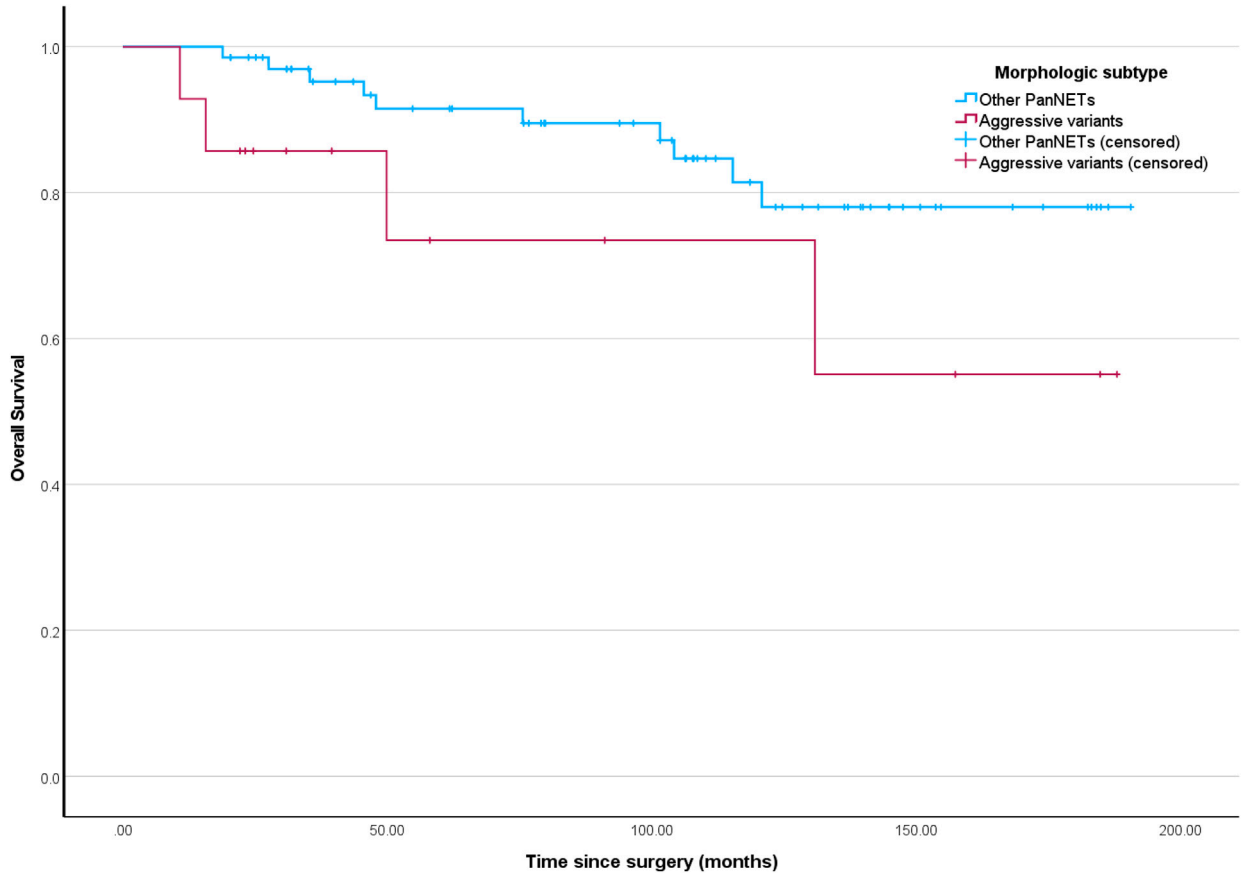


FIGURE 5
Kaplan-Meier overall survival curves for pancreatic neuroendocrine tumors, stratified by morphologic variant (aggressive vs. others). The aggressive variant group showed a numerically shorter overall survival time, although the difference did not reach statistical significance (log-rank $p = 0.086$).

TABLE 3 **Univariable Cox regression analyses for OS and RFS.**

Variable	OS (HR, 95% CI, p)	RFS (HR, 95% CI, p)
Aggressive variant (vs. other)	2.66 (0.83–8.54), $p = 0.099$	0.96 (0.22–4.29), $p = 0.958$
Aggressive + indeterminate variant (vs. other)	1.55 (0.48–4.94), $p = 0.462$	1.09 (0.31–3.89), $p = 0.890$
Aggressive variant ≥50% (vs. other)	2.81 (0.88–9.00), $p = 0.081$	1.06 (0.24–4.74), $p = 0.938$
Grade 3 (vs. Grade 1–2)	4.18 (0.89–19.58), $p = 0.069$	4.94 (1.08–22.64), $p =$ **0.040**
pT3–4 (vs. pT1–2)	2.37 (0.77–7.29), $p = 0.133$	3.20 (1.10–9.28), $p =$ **0.033**
Nodal status (N1 vs. N0)	3.42 (1.00–11.77), $p = 0.051$	5.33 (1.67–17.01), $p =$ **0.005**
Tumor size >2 cm	2.42 (0.67–8.79), $p = 0.180$	3.38 (0.95–12.00), $p = 0.060$
Tumor size (per 1 cm increase)	–	1.15 (1.00–1.33), $p =$ **0.045**
Ki-67 index (per 1% increase)	1.05 (1.02–1.09), $p =$ **0.002**	1.08 (1.03–1.13), $p =$ **0.001**
R1 margin (vs. R0)	–	1.46 (0.46–4.61), $p = 0.523$
Lymphovascular invasion	–	3.28 (1.09–9.87), $p =$ **0.035**
Perineural invasion	–	2.78 (0.96–8.08), $p = 0.060$

Univariable Cox regression analyses were performed separately for OS and RFS. Statistically significant p-values (<0.05) are shown in bold. OS, overall survival; RFS, recurrence-free survival; HR, hazard ratio; CI, confidence interval. The ≥50% threshold for aggressive variant morphology was evaluated in an additional sensitivity analysis.

significant difference in RFS between aggressive morphologic variants and other PanNETs (log-rank $p = 0.958$). In a sensitivity analysis that included indeterminate variants in the aggressive group, the results remained unchanged (log-rank $p = 0.890$). In contrast, RFS differed significantly according to established clinicopathologic parameters. Patients with grade 3 tumors (vs. grade 1–2), advanced pT stage, and node-positive disease showed significantly poorer RFS (log-rank $p = 0.023$, $p = 0.024$, and $p = 0.002$, respectively).

In univariable Cox regression analyses, including the sensitivity model incorporating indeterminate variants within the aggressive group, grade 3 tumors (vs. grade 1–2), advanced pT stage, nodal involvement, LVI, an increased Ki-67 index (per 1% increase), and tumor size analyzed as a continuous variable were associated with an increased risk of recurrence, whereas morphologic variant status, surgical margin status, PNI, and tumor size dichotomized at a 2-cm cutoff were not significantly associated with RFS (Table 3).

In the first multivariable Cox regression model, adjusted for univariable significance and biological relevance, nodal involvement remained independently associated with an increased risk of recurrence (HR 4.41; 95% CI 1.35-14.38; $p = 0.014$). While pT stage did not retain statistical significance, the Ki-67 index showed a trend toward an increased risk of recurrence, although the association did not reach statistical significance (HR 1.05; 95% CI 1.00–1.10; $p = 0.060$) (Supplementary Table S1, Model 1).

In a separate, hypothesis-driven, multivariable model that evaluated the independent impact of morphology, morphologic variant status was not significantly associated with RFS (HR 0.63; 95% CI 0.11-3.54; $p = 0.597$). In this model, nodal status remained independently associated with recurrence risk (HR 4.86; 95% CI 1.48-16.01; $p = 0.009$), whereas Ki-67 was not independently associated with RFS, although the point estimate suggested a possible association (HR 1.05; 95% CI 1.00-1.11; $p = 0.054$) (Supplementary Table S1, Model 2).

In an additional sensitivity analysis applying a ≥50% threshold for aggressive variant morphology, the RFS findings remained unchanged, with no statistically significant difference between aggressive variants and other tumors (log-rank $p = 0.938$; univariable Cox HR = 1.06, 95% CI 0.24–4.74, $p = 0.938$) (Table 3).

Overall, morphologic variant status did not demonstrate an independent impact on recurrence risk in either the primary or sensitivity models.

Discussion

The present study retrospectively evaluated 82 resected, well-differentiated PanNETs from a single institution, identified morphologic variants using literature-based criteria, and examined their associations with clinicopathologic parameters and survival outcomes, with a particular focus on variants previously linked to aggressive behavior.

In our cohort, nearly one-quarter of tumors exhibited non-classical morphologic features, a frequency comparable to previous large-scale series [1]. The spectrum of variants largely overlapped with those described in prior studies, supporting the reproducibility of these morphologic patterns in routine practice [1, 6, 13, 14, 17, 22, 30, 31]. Notably, several variants reported in the literature, such as ductuloinsular, mammary tubulo-lobular carcinoma-like, and sclerosing patterns, were not observed in our cohort, likely reflecting their extreme rarity rather than their true absence [1, 4, 5].

Oncocytic and hepatoid morphologies have been described as distinct PanNET variants based on architectural, cytologic, immunophenotypic, and ultrastructural features, including mitochondria-rich eosinophilic cytoplasm and, in hepatoid cases, a higher nuclear-to-cytoplasmic ratio, cytoplasmic lipid-like deposits, and hepatocellular marker expression [1, 14–17, 32]. Previous studies have also associated these morphologies with more aggressive clinicopathologic features [1, 17]. A more recent review of the literature by Xue and Reid, who were involved in the original characterization of these categories, now considers hepatoid morphology a subtype within the broader oncocytic spectrum rather than a distinct variant, based on their shared eosinophilic cytoplasm and overlapping morphologic features [32]. In our cohort, tumors with abundant eosinophilic cytoplasm similarly showed overlapping oncocytic and hepatoid features, with variable, often focal hepatocellular marker expression and no steatosis. In keeping with emerging literature and their broadly similar clinicopathologic behavior, these findings support interpreting such tumors as part of an eosinophilic morphologic spectrum rather than as rigidly distinct entities.

In the dyscohesive/plasmacytoid-rhabdoid variant, ultrastructural studies have shown that the intracytoplasmic globules underlying rhabdoid morphology correspond to paranuclear aggregates of intermediate filaments and may coexist with conventional neuroendocrine areas, supporting the interpretation of this pattern as a morphologic phenotype within the PanNET spectrum rather than a distinct entity [26, 27]. Solid pseudopapillary neoplasm-like architecture, described in a subset of cases [1], was not observed in our cohort.

The lipid-rich (clear cell) variant is a rare but well-recognized morphologic pattern. Although historically linked to von Hippel-Lindau syndrome, similar features have also been reported in sporadic PanNETs [6, 9, 11, 12]. In our cohort, which excluded syndromic cases, lipid-rich morphology was identified in two tumors, supporting its occurrence in sporadic PanNETs. We also observed focal clear cell-like changes adjacent to fibrotic areas, likely related to prior fine-needle aspiration, in otherwise conventional PanNETs, highlighting a potential diagnostic pitfall and emphasizing the importance of distinguishing true lipid-rich changes from reactive or procedure-related cytoplasmic clearing. The peliotic/angiomatoid and pseudoglandular variants are uncommon morphologic patterns, with limited data, and their clinicopathologic significance remains uncertain [1].

The paraganglioid variant is rare and represents a well-recognized diagnostic challenge due to its resemblance to paraganglioma [1, 30]. In our cohort, this variant was identified in two cases, one of which demonstrated prominent pleomorphic (symplastic) tumor cells, a feature described both in paraganglioid PanNETs and as a distinct pleomorphic PanNET variant [1, 21]. Such pleomorphism may further complicate diagnosis by mimicking high-grade carcinoma despite preserved well-

differentiated neuroendocrine features and low proliferative activity. Although S100-positive sustentacular cells have been reported in some cases, this finding is inconsistent and typically less prominent than in true paragangliomas [1, 30]. In our cases, a sustentacular staining pattern was not identified; instead, diffuse S100 positivity was observed within tumor cells, further supporting their epithelial neuroendocrine differentiation rather than a true paraganglionic lineage.

From a diagnostic perspective, these morphologic variants represent important pitfalls, particularly in limited biopsy or metastatic settings. Eosinophilic tumors may mimic hepatocellular or oncocytic neoplasms; dyscohesive/plasmacytoid variants may resemble poorly cohesive/signet-ring cell carcinoma and hematolymphoid malignancies; lipid-rich tumors may simulate clear cell neoplasms, including adrenocortical tumors and clear cell renal cell carcinomas; pseudoglandular tumors may mimic adenocarcinoma; and paraganglioid tumors may be confused with paraganglioma. A lack of awareness of these morphologic variants may lead to the exclusion of neuroendocrine tumors from the differential diagnosis, resulting in misdiagnosis and inappropriate clinical management. Careful cytologic assessment, recognition of residual conventional PanNET areas, and confirmation with neuroendocrine markers are therefore essential for an accurate diagnosis in both primary and metastatic settings.

From a clinicopathologic standpoint, morphologic variants previously categorized as more aggressive in the literature were associated with higher Ki-67 indices and higher WHO grades in our cohort, consistent with increased proliferative activity. Tumors with these morphologic patterns showed a trend toward larger tumor size, although the difference did not reach statistical significance. These findings are broadly consistent with previous reports describing associations between selected morphologic variants and adverse histopathologic features [1, 14]. A prior study also reported higher rates of nodal and metastatic adverse events among aggressive variants [1]. We did not observe significant associations between morphologic variant status and nodal involvement or distant metastatic disease at diagnosis. This difference may reflect differences in cohort composition, endpoint definitions, and limited statistical power. Notably, aggressive morphologic variants were also more frequent in male patients, consistent with prior reports; although the biological basis of this association remains unclear [1, 14].

Despite their association with adverse histopathologic features, morphologic variants previously categorized as aggressive were not significantly associated with OS or RFS in our cohort, although a trend toward a less favorable OS was observed. Established prognostic parameters, including the Ki-67 index and nodal status, showed associations with recurrence outcomes, with nodal status remaining independently associated in multivariable analysis. Notably, while the Ki-67 index did not reach conventional statistical significance in the multivariable models, its point estimate suggested a possible association with poorer RFS. This finding is consistent with the established prognostic role of proliferative activity in PanNETs, although confirmation in larger cohorts with greater event numbers is warranted. However, Xue et al. reported higher rates of adverse outcomes among morphologic variants categorized as aggressive in their study [1]. Differences between studies may partly reflect methodological variations, as that study assessed composite adverse outcome measures that incorporated nodal, metastatic, and follow-up adverse events, whereas our study evaluated conventional time-to-event endpoints. Nevertheless, the limited number of variant cases and survival events in our cohort restricts definitive conclusions regarding the prognostic significance of specific morphologic variants, which should be further evaluated in larger, multi-institution cohorts.

The lipid-rich variant warrants particular mention, as it has been categorized among aggressive morphologies in prior reports based on descriptions of adverse outcomes despite low Ki-67 indices [1]. In our cohort, lipid-rich tumors similarly demonstrated a low proliferation profile (grade 1-2; median Ki-67 index, 3%). Both tumors were small (1.2 and 2.5 cm); neither showed distant metastasis, and no recurrence occurred during prolonged follow-up (approximately 4.8 and 7.6 years), despite one case being node-positive. Although no adverse outcomes were observed in our limited number of cases, the small sample size precludes definitive conclusions regarding the prognostic behavior of lipid-rich PanNETs. Variability in tumor size, stage distribution, and statistical power may partly explain the prognostic discrepancies reported across studies.

Similarly, morphologic variants categorized as indeterminate, particularly the peliotic/angiomatoid pattern (three cases), did not demonstrate an overtly aggressive clinical course in our cohort, although case numbers were limited, and only a single recurrence without disease-related death was observed. These observations further underscore the heterogeneity of morphologic variants and suggest that non-classical morphologic patterns may not uniformly correspond to similar clinicopathologic behavior. Taken together, our findings support the classification of morphologic variants as a useful component of histopathologic characterization, while suggesting that their prognostic significance should be interpreted cautiously and in the context of established clinicopathologic parameters.

The strengths of the present study include a well-characterized cohort of resected PanNETs with a detailed histopathologic review, long-term follow-up, and a systematic assessment of morphologic variants using classification based on previously published criteria. Unlike prior studies, we evaluated OS and RFS as conventional time-to-event outcomes, allowing assessment of prognostic associations beyond composite metastatic outcome measures. However, several limitations should be acknowledged. This was a retrospective single-institution study with a limited number of morphologic variant cases, reflecting the rarity of these patterns in resected PanNET cohorts and restricting statistical power for subgroup analyses. In addition, the relatively low number of recurrence and survival events may have reduced the sensitivity in detecting subtle or borderline prognostic effects of morphologic variant status. Finally, more granular outcome measures, such as disease-specific survival or separate analyses of locoregional versus distant recurrence, were not evaluated.

In conclusion, morphologic variants of PanNETs represent an important component of the histologic spectrum of PanNETs and are associated with distinct clinicopathologic features. Recognition of these variants remains important in diagnostic practice, particularly in limited biopsy or metastatic settings where they may mimic other neoplasms. While certain morphologic patterns were associated with adverse histopathologic features in our cohort, their prognostic significance remains uncertain and should be

interpreted cautiously in the context of established clinicopathologic parameters such as nodal status and proliferation index. Larger, multi-institutional studies with greater numbers of variant cases and outcome events are needed to better clarify the prognostic relevance of specific morphologic variants.

Data availability statement

The original contributions presented in the study are included in the article/Supplementary Material, further inquiries can be directed to the corresponding author.

Ethics statement

The studies involving humans were approved by Istanbul University Istanbul Faculty of Medicine Clinical Research Ethics Committee. The studies were conducted in accordance with the local legislation and institutional requirements. The ethics committee/institutional review board waived the requirement of written informed consent for participation from the participants or the participants' legal guardians/next of kin because of the retrospective design of the study and the use of anonymized archival data.

Author contributions

NB, MB, and MG conceived and designed the study. NB, BG, and KS collected the data. NB, MB, and MG performed data analysis and interpretation. NB performed the statistical analysis and drafted the manuscript. MB and MG critically revised the manuscript. MG supervised the study. All authors contributed to the article and approved the submitted version.

Funding

The author(s) declared that financial support was not received for this work and/or its publication.

Acknowledgments

Preliminary findings related to this work were presented as an oral presentation at the 33rd National Pathology Congress (November 2024, Antalya, Turkey).

Conflict of interest

The author(s) declared that this work was conducted in the absence of any commercial or financial relationships that could be construed as a potential conflict of interest.

Generative AI statement

The author(s) declared that generative AI was not used in the creation of this manuscript.

Any alternative text (alt text) provided alongside figures in this article has been generated by Frontiers with the support of artificial intelligence and reasonable efforts have been made to ensure accuracy, including review by the authors wherever possible. If you identify any issues, please contact us.

Supplementary material

The Supplementary Material for this article can be found online at: https://www.por-journal.com/articles/10.3389/pore.2026.1612573/full#supplementary-material

References

1. Xue Y, Reid MD, Pehlivanoglu B, Obeng RC, Jiang H, Memis B, et al. Morphologic variants of pancreatic neuroendocrine tumors: clinicopathologic analysis and prognostic stratification. *Endocr Pathol* (2020) 31(3):239–53. doi: 10.1007/s12022-020-09628-z

2. Mattiolo P, Scarpa A, Luchini C. Hepatoid tumors of the gastrointestinal/pancreatobiliary district: morphology, immunohistochemistry, and molecular profiles. *Hum Pathol* (2023) 132:169–75. doi: 10.1016/j.humpath.2022.06.011

3. Miyazaki T, Aishima S, Fujino M, Ozono K, Kubo Y, Ushijima Y, et al. Neuroendocrine tumor of the pancreas with rhabdoid feature. *Virchows Arch* (2018) 473(2):247–52. doi: 10.1007/s00428-018-2398-x

4. van Eeden S, de Leng WW, Offerhaus GJ, Morsink FH, Weterman MA, de Krijger RR, et al. Ductuloinsular tumors of the pancreas: endocrine tumors with entrapped nonneoplastic ductules. *Am J Surg Pathol* (2004) 28(6):813–20. doi: 10.1097/01.pas.0000112546.57641.c7

5. Deshpande V, Selig MK, Nielsen GP, Fernandez-del Castillo C, Lauwers GY. Ductulo-insular pancreatic endocrine neoplasms: clinicopathologic analysis of a unique subtype of pancreatic endocrine neoplasms. *Am J Surg Pathol* (2003) 27(4):461–8. doi: 10.1097/00000478-200304000-00005

6. Xia R, Tang LH, Shafizadeh N, Xue Y, Liu X. Unveiling lipid-rich ("clear cell") pancreatic neuroendocrine tumor: a small series of two cases with literature review. *Diagn Cytopathol* (2024) 52(10):582–8. doi: 10.1002/dc.25296

7. Shattuck TM, Waugh MS. Lipid-rich variant of a pancreatic endocrine neoplasm in an endoscopic ultrasound-guided fine needle aspiration biopsy. *Diagn Cytopathol* (2013) 41(8):703–4. doi: 10.1002/dc.22853

8. Rao AC, Monappa V, Shetty P. Lipid-rich variant of pancreatic endocrine tumour with inhibin positivity and microscopic foci of microcystic adenoma-like areas: emphasis on histopathology. *Singapore Med J* (2013) 54(2):e31–4. doi: 10.11622/smedj.2013036

9. Fryer E, Serra S, Chetty R. Lipid-rich ("clear cell") neuroendocrine tumors of the pancreas in MEN I patients. *Endocr Pathol* (2012) 23(4):243–6. doi: 10.1007/s12022-012-9221-z

10. Ayub SB, Dodge J. Lipid-rich variant of pancreatic endocrine neoplasms: a case report. *Acta Cytol* (2010) 54(5 Suppl. l):829–34.

11. Singh R, Basturk O, Klimstra DS, Zamboni G, Chetty R, Hussain S, et al. Lipid-rich variant of pancreatic endocrine neoplasms. *Am J Surg Pathol* (2006) 30(2):194–200. doi: 10.1097/01.pas.0000184819.71752.ad

12. Hoang MP, Hruban RH, Albores-Saavedra J. Clear cell endocrine pancreatic tumor mimicking renal cell carcinoma: a distinctive neoplasm of von Hippel-Lindau disease. *Am J Surg Pathol* (2001) 25(5):602–9. doi: 10.1097/00000478-200105000-00006

13. Ordonez NG, Silva EG. Islet cell tumour with vacuolated lipid-rich cytoplasm: a new histological variant of islet cell tumour. *Histopathology* (1997) 31(2):157–60. doi: 10.1046/j.1365-2559.1996.2230837.x

14. Hsiao WY, O'Brien SM, Rajack F, Tadros T, Reid MD. Oncocytic subtype of well-differentiated neuroendocrine tumor: clinicopathologic and molecular associations of a cohort diagnosed on fine needle aspiration (FNA). *J Am Soc Cytopathol* (2025) 14(4):209–21. doi: 10.1016/j.jasc.2025.03.004

15. Di Carlo S, Zaitoun A, Fielding D, Gomez D. Oncocytic neuroendocrine tumour of the pancreas and duodenum: two case reports with review of the literature. *JOP: J Pancreas* (2015) 16(4):380–3.

16. Chen S, Wang X, Lin J. Fine needle aspiration of oncocytic variants of pancreatic neuroendocrine tumor: a report of three misdiagnosed cases. *Acta Cytol* (2014) 58(2): 131–7. doi: 10.1159/000357035

17. Volante M, La Rosa S, Castellano I, Finzi G, Capella C, Bussolati G. Clinico-pathological features of a series of 11 oncocytic endocrine tumours of the pancreas. *Virchows Arch* (2006) 448(5):545–51. doi: 10.1007/s00428-006-0154-0

18. Chetty R, Kennedy M, Ezzat S, Asa SL. Pancreatic endocrine pathology in von Hippel-Lindau disease: an expanding spectrum of lesions. *Endocr Pathol* (2004) 15(2): 141–8. doi: 10.1385/ep:15:2:141

19. Nguyen-Ho P, Nguyen GK, Jewell LD. Oncocytic neuroendocrine carcinoma of the pancreas. Report of a case with needle aspiration cytology, immunocytochemistry and electron microscopy. *Acta Cytol* (1994) 38(4):611–3.

20. Carstens PH, Cressman FK, Jr. Malignant oncocytic carcinoid of the pancreas. *Ultrastruct Pathol* (1989) 13(1):69–75. doi: 10.3109/01913128909051162

21. Zee SY, Hochwald SN, Conlon KC, Brennan MF, Klimstra DS. Pleomorphic pancreatic endocrine neoplasms: a variant commonly confused with adenocarcinoma. *Am J Surg Pathol* (2005) 29(9):1194–200. doi: 10.1097/01.pas.0000164370.81132.25

22. Fite JJ, Ali SZ, VandenBussche CJ. Fine-needle aspiration of a pancreatic neuroendocrine tumor with prominent rhabdoid features. *Diagn Cytopathol* (2018) 46(7):600–3. doi: 10.1002/dc.23892

23. Shia J, Erlandson RA, Klimstra DS. Whorls of intermediate filaments with entrapped neurosecretory granules correspond to the "rhabdoid" inclusions seen in pancreatic endocrine neoplasms. *Am J Surg Pathol* (2004) 28(2):271–3. doi: 10.1097/00000478-200402000-00018

24. Perez-Montiel MD, Frankel WL, Suster S. Neuroendocrine carcinomas of the pancreas with 'rhabdoid' features. *Am J Surg Pathol* (2003) 27(5):642–9. doi: 10.1097/00000478-200305000-00007

25. Stokes MB, Kumar A, Symmans WF, Scholes JV, Melamed J. Pancreatic endocrine tumor with signet ring cell features: a case report with novel ultrastructural observations. *Ultrastruct Pathol* (1998) 22(2):147–52. doi: 10.3109/01913129809032270

26. Chetty R, Asa SL. Pancreatic endocrine tumour with cytoplasmic keratin whorls. Is the term "rhabdoid" appropriate? *J Clin Pathol* (2004) 57(10):1106–10. doi: 10.1136/jcp.2004.018309

27. Serra S, Asa SL, Chetty R. Intracytoplasmic inclusions (including the so-called "rhabdoid" phenotype) in pancreatic endocrine tumors. *Endocr Pathol* (2006) 17(1): 75–81. doi: 10.1385/ep:17:1:75

28. WHO Classification of Tumours Editorial Board. *Endocrine and Neuroendocrine Tumours*. 5 ed. Lyon: International Agency for Research on Cancer (2022).

29. American Joint Committee on Cancer. *AJCC Cancer Staging Manual*. 8 ed. New York: Springer (2017).

30. Konukiewitz B, von Hornstein M, Jesinghaus M, Steiger K, Weichert W, Detlefsen S, et al. Pancreatic neuroendocrine tumors with somatostatin expression and paraganglioma-like features. *Hum Pathol* (2020) 102:79–87. doi: 10.1016/j.humpath.2020.07.004

31. Reid MD, Balci S, Saka B, Adsay NV. Neuroendocrine tumors of the pancreas: current concepts and controversies. *Endocr Pathol* (2014) 25(1):65–79. doi: 10.1007/s12022-013-9295-2

32. Xue Y, Reid MD. Well-differentiated pancreatic neuroendocrine tumor: does morphologic variant matter? *Arch Pathol Lab Med* (2025) 150:e123–e130. doi: 10.5858/arpa.2025-0034-RA